Biosensors and Bioelectronics 130 (2019) 40–47

Contents lists available at ScienceDirect

Biosensors and Bioelectronics

journal homepage: www.elsevier.com/locate/bios

Gold-nanorod enhances dielectric voltammetry detection of c-reactive protein: A predictive strategy for cardiac failure

Iswary Letchumanan[a], M.K. Md Arshad[a,b], S.R. Balakrishnan[c], Subash C.B. Gopinath[a,d,*]

[a] Institute of Nano Electronic Engineering, Universiti Malaysia Perlis, 01000 Kangar, Perlis, Malaysia
[b] School of Microelectronic Engineering, Universiti Malaysia Perlis, Pauh Putra, Arau 02600, Perlis, Malaysia
[c] Fakulti Kejuruteraan dan Alam Bina, Universiti Sains Islam Malaysia, Bandar Baru Nilai, 71800 Nilai, Negeri Sembilan, Malaysia
[d] School of Bioprocess Engineering, Universiti Malaysia Perlis, 02600 Arau, Perlis, Malaysia

ARTICLE INFO

Keywords:
C-reactive protein
Gold nanorod
Nanogapped sensor
Voltammetry

ABSTRACT

This paper primarily demonstrates the approach to enhance the sensing performance on antigen C-reactive protein (CRP) and anti-CRP antibody binding event. A nanogapped electrode structure with the gap of ~100 nm was modified by the anti-CRP antibody (Probe) to capture the available CRP. In order to increase the amount of antigen to be captured, a gold nanorod with 119 nm in length and 25 nm in width was integrated, to increase the surface area. A comparative study between the existence and non-existence of gold nanorod utilization was evaluated. Analysis of the sensing surface was well-supported by atomic force microscopy, scanning electron microscopy, 3D nano-profilometry, high-power microscopy and UV–Vis spectroscopy. The dielectric voltammetric analysis was carried out from 0 V to 2 V. The sensitivity was calculated based on 3σ and attained as low as 1 pM, which is tremendously low compared to real CRP concentration (119 nM) in human blood serum. The gold nanorod conjugation with antibody has enhanced the sensitivity to 100 folds (10 fM). The specificity of the CRP detection by the proposed strategy was anchored by ELISA and failure in the detection of human blood clotting factor IX by voltammetry. Despite, CRP antigen was further detected in human serum by spiking CRP to run-through the detection with the physiologically relevant samples.

1. Introduction

Cardiovascular diseases (CVD) is the dominant cause for the morbidity and mortality worldwide (Fonseca et al., 2016). Fortunately, research conjugating the discovery of biomarkers could ease the early detection and prediction of diseases which is much needed for the precaution measurements with CVD risks (Gupta et al., 2014). Several common biomarkers are engaged with CVD risks, such as troponin-T and -I, Myosin light chain kinase 1 for a myocardial infarction while C-reactive Protein (CRP) for inflammation (Keen and Gables, 2016; Md Arshad et al., 2016). CRP is acute phase protein produced by the liver which able to increase the level within a few hours after inflammation process. In a healthy individual the CRP concentrations vary between 0.8 and 3 mg/L. Generally, three proposed CRP levels in human serum are, low-risk (1 mg/L), average-risk (1–3 mg/L) and high-risk (> 3 mg/L) (Md Arshad et al., 2016). CRP test utilizing patient serum (Cheen et al., 2017) is needed to verify if an individual has a problem linked to acute infection or inflammation. Despite inflammation, bacterial and viral infections are also causing to rise the CRP level. Albeit biomarker finding, the best detection method is must in order to reduce the fatality rate. Although, the standard 12-lead electrocardiogram is currently the preferred test to recognize patients with acute CVD, due to its poor sensitivity the additional diagnostic techniques are mandatory (Fathil et al., 2015).

Nanotechnology plays a significant role in revolutionizing the efficiency of biosensor predominantly in the medical field (Pundir and Narwal, 2018). Nanoparticles are most extensively used for the betterment and the precise biomolecule detection. Moreover, nanoparticles are useful for early detection, which are eligible to utilize in medical diagnosis (Pandit et al., 2016). Gold nanomaterial, such as gold nanorod (GNR) has a promising effect on improving the sensing platform. Gold nanomaterial promote greater abilities of binding the biomolecules (Gopinath et al., 2017), due to its outstanding physiochemical properties such as a large surface area, better conductivity, biocompatibility and improves the limit of detection (Xu et al., 2017). Concerning the conventional techniques that were practiced last decades to detect CRP in clinical laboratories, they consume huge amount and expensive reagents in every assay and may take several hours or

* Corresponding author at: Institute of Nano Electronic Engineering, Universiti Malaysia Perlis, 01000 Kangar, Perlis, Malaysia.
E-mail address: subash@unimap.edu.my (S.C.B. Gopinath).

https://doi.org/10.1016/j.bios.2019.01.042
Received 1 October 2018; Received in revised form 26 December 2018; Accepted 14 January 2019
Available online 29 January 2019
0956-5663/

even days to receive the consolidated results. ELISA is a 'gold standard' strategy, broadly utilized to detect the antigen causing disease by using the suitable antibody. This experiment was performed in this study to prove the presented sensor displays a higher sensitivity compared to the ELISA and to confirm the genuine interaction of CRP-antigen and its antibody. ELISA has a higher specificity but with a lower sensitivity, able to detect at the nanomolar range in general, whereby the proposed sensor has the limit of detection as low as 10 fM. ELISA is still performing well in the detection of CRP but the usage become limited due to expensive and the trained personnel needed to perform the method. Despite amount requirement and high cost, the detection limit is still high where the accuracy level is low. Engage in this issue, doctors unable to make a quick decision which is incompatible to treat high-risk CVD patients.

To overwhelm these limitations, the biosensor-based strategy has been proposed for the detection of CRP biomarkers (Fathil et al., 2016). Furthermore, it is a suitable device for early diagnosis because of their low level of detection limits in physiological samples. For the current study, the antigen (CRP) was immobilized on GNR to develop the detection on the nano gapped electrode. A clear-cut comparison was carried out between the presence and absence of GNR integration during the detection of the antigen-antibody coupling event. The current to voltage (I-V) measurements were performed to analyze the current flow. Furthermore, better performing biosensor can reveal the outstanding outcomes in medical diagnosis because quick accurate outcomes are significant considerations in this field (Sharifi et al., 2018). Engaging to that, several vital factors have been taken into the consideration, which includes the higher number of immobilized biomolecules on sensing surface and reducing the non-specific binding as demonstrated in (Lakshmipriya et al., 2013). To achieve the notions, in the current study, a voltammetry-based dielectric biosensing system was utilized to analyze CRP using the antibody as a probe for the efficient detection of CRP in order to predict the heart failure.

2. Material and methods

2.1. Materials and reagents

C-reactive protein and monoclonal anti-CRP antibody produced in mouse were purchased from BITA LIFESCIENCE Sdn. Bhd. (Malaysia). 3-Aminopropyltriethoxysilane (APTES) was procured from Sigma Aldrich (USA) for nanogapped surface functionalization. Glutaraldehyde solution (50%) was obtained from Sigma Aldrich (USA) for immobilization purpose. Phosphate Buffer Solution from Sigma Aldrich (USA) was utilized as a washing buffer. Ethanolamine from Fisher Scientific (UK) was used as the blocking agent. Gold nanorod was procured from Nanopartz Inc. (USA) to lower the limit of detection. Human serum was purchased from- Sigma Aldrich (USA) for the specificity analysis. N-Hydroxysuccinimide (NHS), 1-Ethyl-3-(3-dimethylaminopropyl) carbodiimide (EDC) and 16-mercaptohexadecanoic acid from GE Healthcare as the cross-linking and stabilizing agents for linking COOH and NH_2. The sensing surface was fabricated as described previously by changing the surface layer and simplified (Balakrishnan et al., 2016).

2.2. Surface functionalization on nanogapped

Initially, the dielectric gap was washed with 70% ethanol and it was dried. Then, 2% of APTES in 30% ethanol was applied onto the surface to create the amine-functionalized substrate and placed for 2 h at room temperature (Balakrishnan et al., 2014). After being washed with PBS and dried, 2.5% of glutaraldehyde was applied on the amine functionalized surface and left for 1 h at room temperature. PBS was used to rinse and remove the unattached molecules from the surface.

2.3. Enzyme-linked immunosorbent assay (ELISA)

To validate the CRP detection using the biosensor possess a lower limit of detection features, different concentrations of CRP were diluted in 1x coating buffer and directly coated onto the ELISA plate surface followed by overnight incubation at 4 °C. Two percent of BSA was used to block the ELISA wells for 1 h to prevent the non-specific binding. The primary anti-CRP antibody with the proper dilution (1:1000) was immobilized onto each well for 2 h. Then, 1:1000 dilution of secondary antibody conjugated HRP was added and incubated for 1 h. A control experiment was carried out using another antigen instead of CRP which is 100 nM of human blood clotting factor IX. Washing steps were performed three times for 10 min between each steps using washing buffer. Finally, the substrate for HRP (Lakshmipriya et al., 2016) was used onto each well to inspect the interaction between CRP and anti-CRP antibody. All the experimental steps were done at ambient temperature. The optical density (OD) reading for the substrate was measured using spectrophotometer and photographs was taken 10 min after the substrate was added.

2.4. Scanning electron microscopy (SEM)

The size of the dielectric gap and GNR was measured using SEM under the accelerated electrons with 20 kV and 50x magnification. GNR was diluted on the bare silicon wafer and blow dried. Later, the sample was observed under SEM with 50x magnification.

2.5. Atomic force microscopy (AFM)

Inspection of the sensing surface morphology before and after the reaction of antigen and antibody was carried out using AFM. AFM demonstrated the resolution at the nanoscale by using beam deflection detection of the devices.

2.6. 3D Surface (Nano) Profilometer

The clear surface morphological difference at the dielectric gap was revealed out by performing the physical characterization test using 3D Surface (Nano) Profilometer. The morphological observation was done before and after the interaction in order to validate the coupling event between antigen and antibody. Surface scanning was performed by controlling PZT with scan rate 13.45 upper limit and 78.67 lower limits. Albeit, 5x magnification was used to obtain a clear-cut image.

2.7. Interaction between anti-CRP antibody and CRP

To interpret the coupling event between anti-CRP-antibody and CRP, the dielectric gap was functionalized as stated above with APTES and glutaraldehyde. Then, 1 μM of anti-CRP-antibody was used constantly for 1 h then washed with PBS followed by 1 M ethanolamine was added for 30 min to block the free surface without anti-CRP antibody immobilized. After that, the surface was washed with PBS. Different concentrations of CRP (100 fM to 10 nM) interacted on the anti-CRP-antibody immobilized surface. All the measurements were carried out using Keithley 6487 picoammeter. All steps were performed at an ambient temperature.

2.8. Interaction between anti-CRP-antibody and gold-conjugated CRP

To mediate the high-performance detection, CRP conjugated gold nanorods (GNRs) interacted on the bound anti-CRP-antibody surface. Thus, the similar surface modification was worked out as mentioned above. Surface with the attached anti-CRP-antibody was tested with different concentrations of CRP-GNP conjugates (100 fM to 10 nM). Samples of CRP-GNP conjugates were prepared initially by premixing GNPs and 16-mercaptohexadecanoic acid for 5 min. Later, 50 mM of N-

Hydroxysuccinimide (NHS) and 200 mM of 1-Ethyl-3-(3-dimethylaminopropyl) carbodiimide (EDC) were mixed with the equal ratio for 10 min followed by interacting CRP for 15 min. Washing and incubation period were exactly followed as mentioned above. Dplot software was used to plot the resultant data in order to analyze the limit of detection.

2.9. Detection of CRP in human serum – Specificity analysis

Surface modified with anti-CRP-antibody was evaluated for the non-specific binding with the blood-related proteins (human clotting factor IX and serum albumin) independently. The concentration of these proteins used was the highest final concentration (100 nM) titrated for the above sensitivity determination. Similarly, the specificity test was carried out using human blood serum with the dilution of 1:1000, dropped on the dielectric gap with anti-CRP-antibody immobilization. Later, 10 fM of CRP was spiked with human serum and added on antibody immobilized nanogapped dielectric sensing surface.

3. Results and discussion

C-reactive protein (CRP) is owned by pentraxin protein family and mainly synthesized in the liver (Adukauskiene et al., 2016). Myocardial infarction and inflammation due to tissue injury, both are highly associated with the elevation of CRP level in human serum because CRP is the key element for inflammatory reaction. Thus, detection of CRP amount in human serum is highly recommended to analyze the disease activity (Ansar and Ghosh, 2013). Different methods have been proposed for varied biomarkers to enhance the sensing mechanism for an instance total internal reflection magnetic imaging combined arrayed 3D photo-magnetic biosensors (Liu et al., 2017) and BioDVD platform (Gopinath et al., 2017). Herein, evidence to up-hold the detection of CRP by its antibody using a nanogapped sensor with the integration of GNR-conjugated CRP is demonstrated. GNR provides more active surface area for the target specific binding to occur, ultimately accommodates higher number of molecules (Fig. 1). Therefore, it may reduce the time consumption to measure antigen-antibody interaction. GNRs have greater absorption and scattering characteristics, which can be a promising tool to boost-up the sensing performance in biological media. GNR was utilized to increase the target-specific binding events to generate high sensitive and precise sensor. Despite, detection of proteins other than CRP was carried out for the specificity analysis and also with the human serum.

3.1. Surface morphology analysis – nanoscale imaging

3.1.1. Sensing surface profiling

Surface morphology of dielectric gap before the coupling event was as presented in (Fig. 2a-d). For this analysis we utilized different microscopic techniques, which include scanning electron microscopy (SEM), 3D nano-profiler, high-power microscopy and atomic force microscopy (AFM). The SEM image apparently shows the nanogap between two electrodes and it was measured to be below 100 nm (Fig. 2a). This result was supported by the image captured from high-power microscopy (Fig. 2b) and image was obtained from 3D nano-profiler (Fig. 2c). Further, we could obtain a clear electrode profile closer to the nanogap under AFM (Fig. 2d). These results demonstrated the clear dielectric profile of the nanogapped sensor has been availed in this study.

3.1.2. Gold nanorod imaging

Similar to the surface morphological analyses on the sensing surface, the GNR to be used for high-performance sensing was also analyzed to reveal its surface morphology and examined under AFM and SEM. Due to the better magnification of AFM, the uniform size distribution of GNR could observe clearly (Fig. 3a). The elongated shape of the GNR increases the surface area and promotes more attachment and interaction of biomolecules to be studied. With the SEM analysis, we could able to capture the image of a single GNR and this observation indicates the length of GNP to be 119 nm and the width is 25 nm (Fig. 3b). These morphological characterizations indicate the capability of GNR to enhance the sensing performance.

3.2. Validation of molecular interactions

3.2.1. UV–Vis spectrophotometry

Generally, protein is made up of several amino acids and the peptide is the combination of several amino acids while polypeptide is a combination of peptide chains. Normally, in liquid-based, protein absorbs ultraviolet light with absorbance maxima close to 280 nm. It is due to the presence of aromatic chains in amino acids causing the absorbance peak to rise to 280 nm (Larson et al., 2018). Aromatic-containing amino acids are able to absorb lights due to the conjugated double bonds. Thus, CRP is also a protein produced by the liver which was utilized in this study, confirmed by the UV–Vis spectrophotometric analysis. A broad absorbance peak for anti-CRP appeared in the range between 200 and 350 nm [Fig. 4a(i)]. The height of the peak was increased further when we measured the CRP [Fig. 4a(ii)]. A drastic enhancement was noticed when we made the complex of GNR-conjugated CRP and anti-

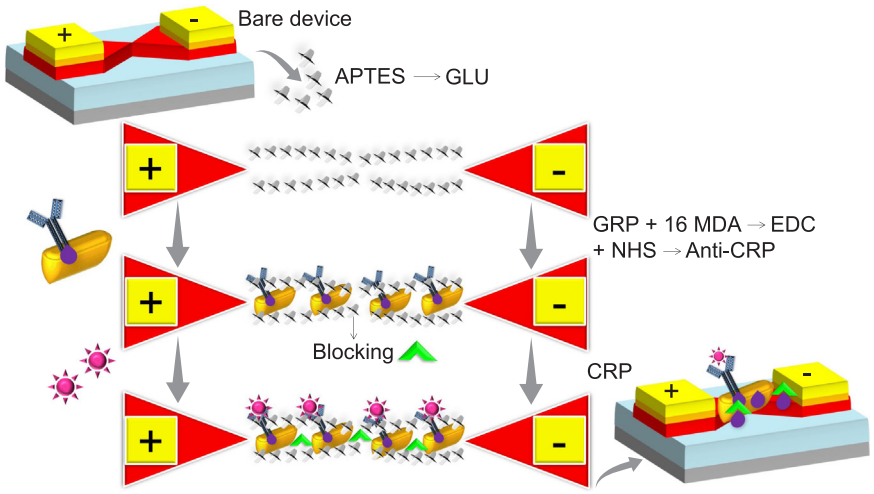

Fig. 1. Schematic illustration for gold-nanorod mediated voltammetry detection of C-reactive protein. Step-by-step molecular attachments are shown.

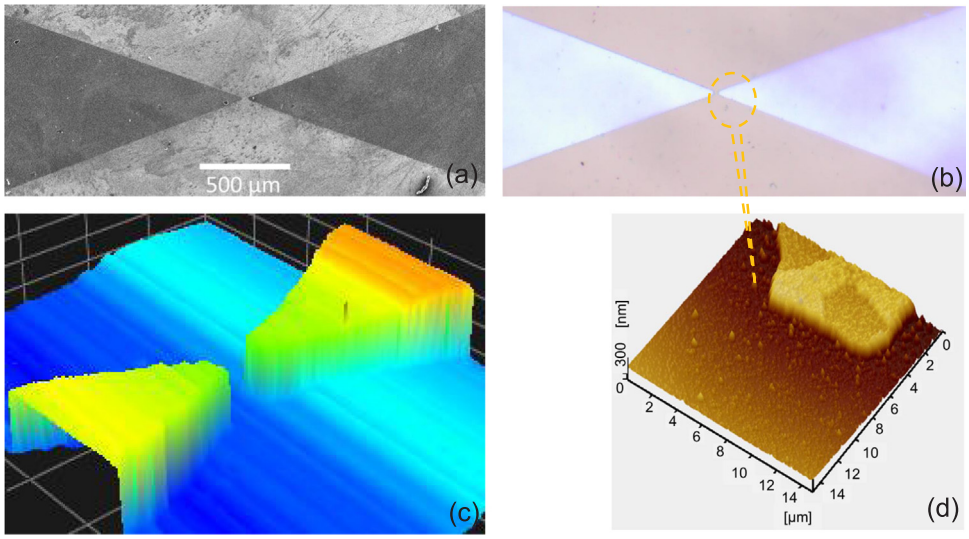

Fig. 2. Surface characterization of the dielectric gapped sensing surface imaging. Scanning Electron Microscopy observation (a); High-power microscopy (b); 3D Surface (Nano) Profilometer (c) and Atomic Force Microscopy (d).

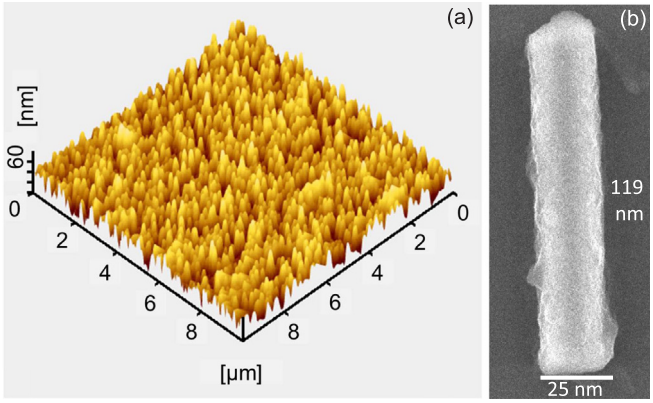

Fig. 3. Morphological characterization for gold nanorod. Atomic Force Microscopy (a) and Scanning Electron Microscopy (b).

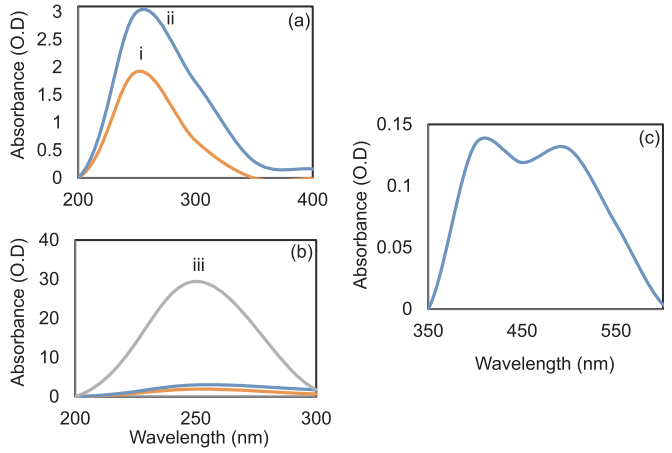

Fig. 4. UV–Vis measurements. Only proteins (a); Proteins and GNR (b); only GNR (c). Anti-CRP-antibody (i); CRP (ii); CRP-GNR complex (iii).

CRP antibody [Fig. 4b(iii)]. On the other hand, when we tested the absorbance of only the GNR, broad and twin-peaks appeared in the range between 350 and 600 nm. In this case, the peaks maximums were recorded at the wavelength 400 and 500 nm (Fig. 4c).

3.2.2. Enzyme-linked immunosorbent assay (ELISA)

ELISA is a complex technique to detect specific protein due to few important considerations that must be emphasized to obtain better results. ELISA is widely considered as the 'gold standard' technique (Poongodi et al., 2002;Lakshmipriya et al., 2016) availed in this study to validate the genuine interaction of CRP and anti-CRP antibody. Herein, target (antigen) was immobilized onto the ELISA wells which create complex between specific capturing agents (antibody) and consequently detected with antibody conjugated with an enzyme. Afterward, the substrate was added on to form enzyme-substrate complex due to the lock and key hypothesis. Therefore, the colour change will occur with the enzymatic reaction and quantitatively measured using UV–vis spectrophotometer at 405 nm (Kim et al., 2018). In this study, different concentrations of CRP antigen (1 fM to 100 nM) was dropped from the lowest to the highest concentration separately into the well, while the negative antigen (Factor IX) and the well without CRP were considered as controls. We observed that a sudden colour change occurs upon adding the substrate to the well with 100 nM antigen concentration. The control wells do not display any changes with the colour. The colour changes were photographed and the absorbance was monitored with each concentration. While no colour changes in other wells mean the absence of the enzymatic reaction. With the 100 nM CRP a prominent peak was recognized under UV–vis spectrophotometry (Fig. 5a), whereby the great absorbance was shown at 100 nM, which predict the detection range began around 100 nM. While no increment at other concentrations is due to the lower concentrations of CRP-antigen, lesser than the detection limit. This result indicates the detection limit is fall in between 10 and 100 nM and it is apparent that with ELISA 100 nM of CRP is necessary for a concrete analysis. Thus, using this level of sensitivity, we further continued the next experiment for the analysis of CRP and anti-CRP antibody interaction using dielectric voltammetry.

3.3. Voltammetry analysis on the interaction of anti-CRP antibody and CRP antigen and sensitivity analysis

Before going for the interactive analysis, the reproducibility of the bare devices was tested by dielectric voltammetry. As shown in Fig. 5b, the I-V responses with different devices are closer and there is no significant difference. With this data, we further proceeded with the dielectric nanogapped sensing analysis. Initially, the surface was chemically functionalized with bifunctional APTES to ease the binding of biomolecules to the silica surface. The existent of an amine group on the surface upon attaching APTES, it facilitates to capture the carboxylic

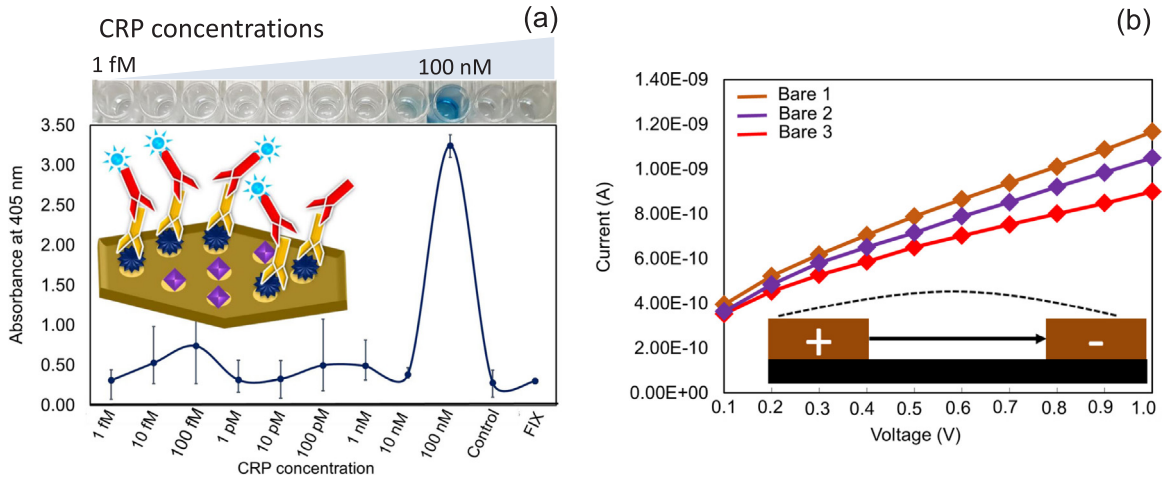

Fig. 5. (a) Enzyme Linked-Immunosorbent Assay. The colour development with the substrate is shown by a photograph. Diagrammatic representation is shown by figure inset. (b) Reproducibility analysis. Three different parallel measurements with bare devices are shown. The dipole moment at the dielectric interface is shown as an inset.

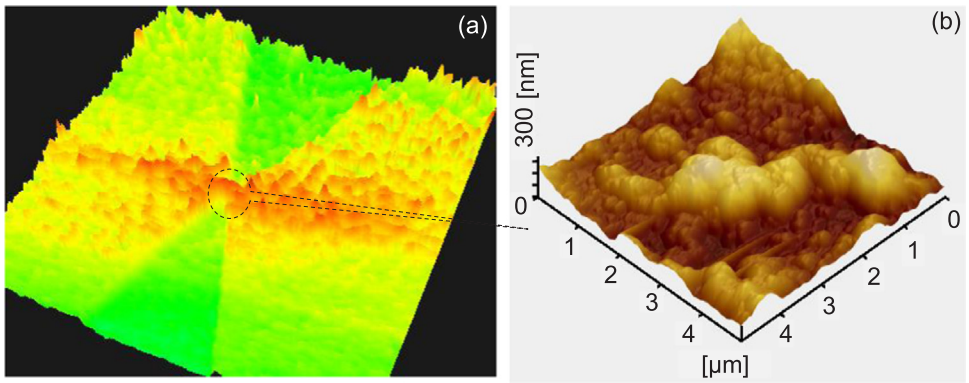

Fig. 6. Surface analysis after the antigen-antibody binding event at the dielectric gapped. 3D Surface (Nano) Profilometer (a); and Atomic Force Microscopy (b).

group-containing molecule, while Si-O group at another end interacts with a silica surface. In current work, glutaraldehyde has been utilized to form a covalent bond with the amine group of APTES. Glutaraldehyde is a linker which owns two aldehyde groups with carbon chain spacer at both ends (Gopinath et al., 2012; Arshad et al., 2018; Victor dos Santos Junior et al., 2018). One of the aldehyde groups reacts with an amine of the APTES while aldehyde at the other end exposed on the surface to interact with the amine group of an antibody. After the glutaraldehyde activation, anti-CRP-antibody was dropped and followed by a blocking with ethanolamine to avoid non-specific biofouling as followed before (Gopinath et al., 2013). On this surface, the higher concentration of CRP observed from the ELISA measurement was used for this initial testing. The surface morphological test was carried out to analyze the reaction occurs between the nanogapped. From this 3D analysis, a clear difference was observed whereby at dielectric gap the colour changes and grown odd structures on the sensing surface, which indicates antigen-antibody coupling event has been occurred (Fig. 6a). Moreover, obvious transformation after the coupling event of antigen and antibody at the dielectric gap was examined visibly through AFM (Fig. 6b).

Initially, the bare device which is absent of any surface chemistry gives the reading of current flow to be 1.8×10^{-6} A followed by the attachment of APTES shows a decrement in current flow as 1.61×10^{-6} A. After the immobilization of anti-CRP-antibody the current decreases to 1.1×10^{-6} A and lower than the bare measurement (Fig. 7a). These changes with different direction are due to the charge variations with the molecules. On this surface, different CRP concentrations were titrated on the anti-CRP immobilized surface, from the lowest concentration at femtomolar to the highest concentration at nanomolar range (10 fM, 100 fM, 1 pM, 10 pM, 100 pM, 1 nM). This measurement was carried out using a Keithley 6487 picoammeter which has two probing system means suitable for the dielectric device. To evaluate the interaction between anti-CRP-antibody and antigen, first 10 fM of CRP was dropped on the dielectric surface then followed by 100 fM and the current flow showed 9×10^{-6} A and 9.15×10^{-6} A. Then, other higher concentrations were titrated consequently, while the current response for 1 pM was 9.18×10^{-6} A and for 10 pM was 9.3×10^{-6} A. Later, 100 pM of CRP was passed on the anti-CRP immobilized surface followed by 1 nM while the current flow showed 9.45×10^{-6} A and 9.9×10^{-6} A respectively (Fig. 7b). Herein, the current flow shows an increment from femto to the picomolar range, however, the current response between the different concentrations almost proceeding towards the sensitivity level of 1 pM based on 3σ calculation (Fig. 7c).

3.4. Voltammetry analysis on the interaction of anti-CRP antibody and gold-nanorod conjugated CRP antigen and sensitivity analysis

The aim of this analysis is to enhance the sensing performance using GNRs and establish by voltammetry measurements of current to voltage (I-V). As stated above GNR with 119 nm length (Fig. 3b) was utilized by functionalizing CRP antigen, and this complex sustains its bioactivity. Gold nanomaterials have been widely utilized for the improvement of the limit of detection in various applications (Gopinath et al., 2013; Lakshmipriya et al., 2016a) Therefore, to create a strong attachment between antigen and GNR, specific cross-linking agent (16-

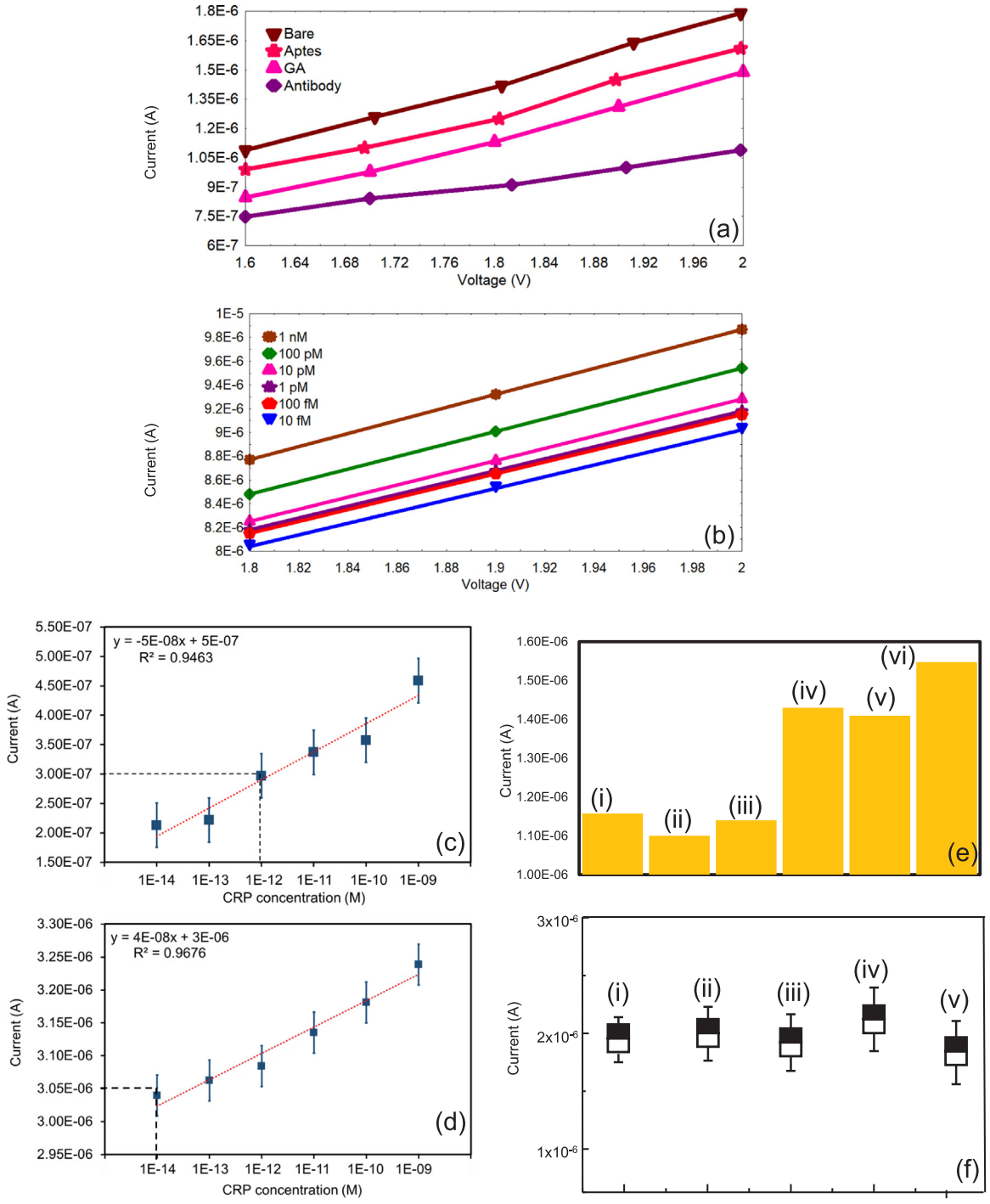

Fig. 7. The current to voltage (I-V) measurements prior to surface modifications (a); Different concentrations of CRP without GNR conjugates (b). Amperometric measurements were performed using 0 V to 2 V at 0.01 V step voltage was used through the analysis. Biomolecular interaction and high-performance analysis with; linear regression analysis for the interaction of CRP and anti-CRP antibody (c); Linear regression analysis for the interaction of CRP-GNR complex and anti-CRP antibody (d); Limit of detection was calculated based on 3σ calculation. Specificity analysis; (e) Specific binding of CRP antibody against different proteins available in human serum was analyzed. Immobilized antibody (i); Factor IX (ii); Serum albumin (iii); C-reactive protein(iv); Human serum (v); Human serum spiked C-reactive protein (vi). The current to voltage (I-V) measurements were performed from 0–2 V whereby the whole calibration plot with 1 V reading was taken. Performance of sensor (f) Stability of the sensor. Bare device (i); APTES (ii); Glutaraldehyde (iii); Anti-CRP antibody (iv); Ethanolamine (v).

mercaptohexadecanoic acid) was integrated to create carboxyl groups on the gold surface, followed by for attaching the antigen EDC and NHS was used. GNR conjugated with a thiol-containing compound from 16-mercaptohexadecanoic acid, and the other end of carboxyl to link amine group. It is necessary to quench EDC and NHS activation reaction with 16-mercaptohexadecanoic acid for 5 min so that EDC binds NHS to carboxyl. EDC is the most outstanding crosslinking agent for biochemical conjugation mechanisms, especially between amine and carboxyl coupling event. Moreover, it also often needed NHS because this conjugation activates the stable binding between molecules. The binding reaction between the cross-linking agent and CRP antigen was 15 min. This mechanism allows for effective coupling event between GNR and CRP antigen. Generally, GNR has awful key characteristics such large surface areas, inertness and better optical properties which

Table 1
Comparison of different sensing strategies for CRP detection.

Method	Material	Probe	Detection limit (pM)	Reference
Photothermal	Platinum	Antibody	3.98	(Lee et al., 2017)
Electrochemical Immunoassay	Screen printed carbon electrode (SPE)	Antibody	150	(Thangamuthu, 2018)
Electrochemical Immunoassay	Screen printed graphene electrode (SPE)	Antibody	59	(Jampasa et al., 2018)
Electrochemical Immunoassay	Zig-zag electrode	Antibody	27	(Kuo et al., 2018)
Impedence spectroscopy	Zinc oxide	Antibody	39	(Cao et al., 2018)
Lossy Mode Resonance (LMR)	Optical fibre	Aptamer	2480	(Zubiate et al., 2017)
Voltammetry	Gold	Antibody	0.01	Current work
ELISA	Polystyrene	Antibody	100000	Current work

are contributing to integrate medical diagnosis for the principal of early and rapid detection. Therefore, GNR was chosen to enhance the sensing performance in this study.

GNR and linking materials were allowed to activate the reaction with different CRP antigen concentrations on the antibody immobilized sensing surface. For the interactive analysis, the same steps as mentioned above experiment were followed. Herein, the above different concentrations of CRP antigen (10 fM, 100 fM, 1 pM, 10 pM, 100 pM, 1 nM) were mixed with GNR. The immobilization was started from the lowest concentration of 10 fM, followed by 100 fM was passed and the current reading was noted to be 9.0×10^{-6} A and 9.2×10^{-6} A. After that, 1 pM, 10 pM and 100 pM were dropped and the current flow was 9.5×10^{-6} A, 9.7×10^{-6} A and 1.0×10^{-5} A respectively. Later, 1 nM of CRP was dropped on the anti-CRP immobilized surface and the current response was 1.2×10^{-5} A. This is due to the resistance increasing during the adding of high concentration samples on the sensing surface leading to the more antigen-antibody binding event. Thus, the barrier to direct current flow along the electrodes increases whereby the resistance also increases. Despite, electrical current changes are with the concomitant changes in the target concentrations, due to the dipole moment at the dielectric interface (Fig. 5b). The dipole moment is induced more when the strong binding event between antigen and antibody occurs, and the formation of the local structure has triggered the vibrations. Thus, these strong charge displacements are causing the electrical current change when the concentration increases. Nevertheless, the interactive analysis for gold conjugated CRP was approached towards 10 fM as the sensitivity level using 3σ calculation. Moreover, it also shows 10 fold drastic enhancement in current response due to the presence of GNR compared to without GNR. Based on the above results, linearity plot (concentration versus current) was plotted to distinguish the performance and stability of the current dielectric device. By interpreting, it was demonstrated that GNR integration is a promising enhancement method to mediated high-performance sensing in clinical diagnosis where the level of sensing performance tremendously increase by 100 folds in GNR conjugated CRP interactive analysis compared to without GNR (Fig. 7d).

3.5. Specificity and stability analyses

Analytical performance for CRP detection on dielectric biosensor was carried out as shown in Fig. 7e&f. The specificity test using different proteins which are abundant in human serum passed independently on the anti-CRP-antibody immobilized surface. In this study, 10 nM of BSA and human blood clotting factor IX (FIX) were used to check the specificity against CRP. Initially, human coagulation FIX was dropped on the surface and the current measurement was recorded. Similarly, serum albumin was deposited on the dielectric sensing surface and measured. The level of the FIX is 3–5 mg/L in healthy human serum, while serum albumin level in the bloodstream is usually as 45 mg/ml (Lakshmipriya et al., 2013). There was no significant difference in current flow with FIX and serum albumin protein from the antibody. FIX protein gives a current reading about 1.58×10^{-6} A while serum albumin reveals out 1.50×10^{-6} A and it shows the least difference between these two proteins and CRP interaction. The current analytical system shows a clear detection by CRP antibody against CRP compared to other proteins from the serum.

CRP does exist in normal human serum in the range of below 3.0 mg/L. In the current study, we also evaluated in the occurrence of human serum, CRP-spiked human serum was tested with the concentrations 10 fM and 100 fM. Human serum alone with 1:1000 dilution was also passed on the CRP antibody immobilized dielectric surface and the current flow shows increment from the antibody. This is due to the CRP-spiked human serum which demonstrates the abundance of CRP in human serum. However, human serum alone shows a reduction in the current flow compared to the CRP alone. CRP with 10 fM and 100 fM concentrations were spiked into a diluted human serum to test the CRP interaction. For 10 fM it gives 1.3×10^{-6} A of current while for 100 fM it was 1.58×10^{-6} A current. This obvious increment might be due to the presence of higher level of CRP in the human serum (Fig. 7e). Stability analysis clearly shows that the sensor utilized in this work holds an equal capability as currently available high-performance devices (Fig. 7f). Based on the above analysis, the dielectric voltammetry analysis for the interaction of CRP and anti-CRP antibody in the occurrence of GNR has shown the superiority and comparable with the currently available sensors (Table 1).

4. Conclusion

Currently, a powerful tool is much needed for the clinical diagnosis to recognize the degree of disease and assist to treat. Early detection is hence greatly desired to reduce the mortality rate among the disease risk population. Moreover, the fast and accurate result is needed for better treatment by the medical department or changing for a better lifestyle. The biosensor is the promising platform which has met with these demands. Albeit, point-of-care (POC) testing in the areas of diagnosing biological markers and diseases in medicine is highly desired. The availability of POC testing might reduce the time-consumption for the treatment, whereby medical practitioners can act and make a decision according to the patient's current condition. The rapid and sensitive POC can be utilized to detect multiple biomarkers using our system with different probes, which could assist to make a decision in a rapid and accurate manner. Thus, here we utilized a sensitive dielectric gapped biosensor for higher accuracy and fast detection of CRP. The foremost advantage of utilization of biosensor in this experiment is to detect a lower amount of target and to obtain most stable surface for antigen-antibody immobilization. Furthermore, sensing strategy using GNR was integrated into this study to increase the sensing performance. Hence, results obtained revealed a drastic increment in sensing activity, whereby the limit of detection achieved was 10 fM while without gold the limit of detection was 1 p.M. Further, this biosensor capable for the detection in human, thus it shows a great increment of current response after the antibody immobilization through the presence of other serum proteins. CRP biosensor shown here will be an effective tool for early detection purpose to cardiovascular disease risk engaged patients.

CRediT authorship contribution statement

Iswary Letchumanan: Conceptualization, Methodology, Data curation, Writing - original draft, Visualization, Investigation. **M.K. Md Arshad:** Validation, Supervision, Writing - review & editing. **S.R. Balakrishnan:** Methodology, Writing - review & editing. **Subash C.B. Gopinath:** Conceptualization, Methodology, Data curation, Visualization, Investigation, Validation, Supervision, Writing - review & editing.

Acknowledgement

This work was supported by the Department of Higher Education, Ministry of Higher Education (MOHE) of Malaysia under the Fundamental Research Grant Scheme (FRGS), grant number 9003-00629.

References

Adukauskiene, D., Čiginskiene, A., Adukauskaite, A., Pentiokiniene, D., Šlapikas, R., Čeponiene, I., 2016. Clinical relevance of high sensitivity C-reactive protein in cardiology. Medicina 52, 1–10. https://doi.org/10.1016/j.medici.2015.12.001.

Ansar, W., Ghosh, S., 2013. C-reactive protein and the biology of disease. Immunol. Res. 56, 131–142. https://doi.org/10.1007/s12026-013-8384-0.

Arshad, M.K.M., Adzhri, R., Fathil, M.F.M., Gopinath, S.C.B., N M, N.M., 2018. Field-effect transistor-integration with TiO2 nanoparticles for sensing of cardiac troponin I biomarker. J. Nanosci. Nanotechnol. 18, 5283–5291. https://doi.org/10.1166/jnn.2018.15419.

Balakrishnan, S.R., Hashim, U., Letchumanan, G.R., Kashif, M., Ruslinda, A.R., Liu, W.W., Veeradasan, P., Haarindra Prasad, R., Foo, K.L., Poopalan, P., 2014. Development of highly sensitive polysilicon nanogap with APTES/GOx based lab-on-chip biosensor to determine low levels of salivary glucose. Sens. Actuators A Phys. 220, 101–111. https://doi.org/10.1016/j.sna.2014.09.027.

Balakrishnan, S.R., Hashim, U., Gopinath, S.C.B., Poopalan, P., Ramayya, H.R., Veeradasan, P., Haarindraprasad, R., Ruslinda, A.R., 2016. Polysilicon nanogap lab-on-chip facilitates multiplex analyses with single analyte. Biosens. Bioelectron. 84, 44–52. https://doi.org/10.1016/j.bios.2015.10.075.

Cao, L., Kiely, J., Piano, M., Luxton, R., 2018. Facile and inexpensive fabrication of zinc oxide based bio-surfaces for C-reactive protein detection. Sci. Rep. 8, 12687. https://doi.org/10.1038/s41598-018-30793-z.

Cheen, O.C., Gopinath, S.C.B., Perumal, V., Arshad, M.K.M., Lakshmipriya, T., Chen, Y., Haarindraprasad, R., Rao, B.S., Hashim, U., Pandian, K., 2017. Aptamer-based impedimetric determination of the human blood clotting factor IX in serum using an interdigitated electrode modified with a ZnO nanolayer. Microchim. Acta 184, 117–125. https://doi.org/10.1007/s00604-016-2001-6.

Fathil, M.F.M., Md Arshad, M.K., Gopinath, S.C.B., Hashim, U., Adzhri, R., Ayub, R.M., Ruslinda, A.R., Nuzaihan, M., Azman, A.H., Zaki, M., Tang, T.H., 2015. Diagnostics on acute myocardial infarction: cardiac troponin biomarkers. Biosens. Bioelectron. 70, 209–220. https://doi.org/10.1016/j.bios.2015.03.037.

Fathil, M.F.M., Md Arshad, M.K., Ruslinda, A.R., Nuzaihan, M., Gopinath, S.C.B., Adzhri, R., Hashim, U., 2016. Progression in sensing cardiac troponin biomarker charge transductions on semiconducting nanomaterials. Anal. Chim. Acta 935, 30–43. https://doi.org/10.1016/j.aca.2016.06.012.

Fonseca, F.A.H., Izar, M.C. de O., 2016. High-sensitivity c-reactive protein and cardiovascular disease across countries and ethnicities. Clinics (Sao Paulo) 71, 235–242. https://doi.org/10.6061/clinics/2016(04)11.

Gopinath, S.C.B., Awazu, K., Fujimaki, M., Shimizu, K., Mizutani, W., Tsukagoshi, K., 2012. Surface functionalization chemistries on highly sensitive silica-based sensor chips. Analyst 137, 3520–3527. https://doi.org/10.1039/c2an35159e.

Gopinath, S.C.B., Awazu, K., Fujimaki, M., Shimizu, K., Shima, T., 2013. Observations of immuno-gold conjugates on influenza viruses using waveguide-mode sensors. PLoS One 8, 1–10. https://doi.org/10.1371/journal.pone.0069121.

Gopinath, S.C.B., Perumal, V., Rao, B.S., Md Arshad, M.K., Voon, C.H., Lakshmipriya, T., Haarindraprasad, R., Vijayakumar, T., Chen, Y., Hashim, U., 2017. Voltammetric immunoassay for the human blood clotting factor IX by using nanogapped dielectrode junctions modified with gold nanoparticle-conjugated antibody. Microchim. Acta 184, 3739–3745. https://doi.org/10.1007/s00604-017-2389-7.

Gupta, R.K., Periyakaruppan, A., Meyyappan, M., Koehne, J.E., 2014. Label-free detection of C-reactive protein using a carbon nanofiber based biosensor. Biosens. Bioelectron. 59, 112–119. https://doi.org/10.1016/j.bios.2014.03.027.

Jampasa, S., Siangproh, W., Laocharoensuk, R., Vilaivan, T., Chailapakul, O., 2018. Electrochemical detection of c-reactive protein based on anthraquinone-labeled antibody using a screen-printed graphene electrode. Talanta 183, 311–319. https://doi.org/10.1016/j.talanta.2018.02.075.

Keen, E.C., Gables, C., 2016. HHS Public Access 37, 6–9. https://doi.org/10.1002/bies.201400152.A.

Kim, M.E., Park, P.R., Na, J.Y., Jung, I., Cho, J.H., Lee, J.S., 2018. Anti-neuroinflammatory effects of galangin in LPS-stimulated BV-2 microglia through regulation of IL-1β production and the NF-κB signaling pathways. Mol. Cell. Biochem. 0, 1–9. https://doi.org/10.1007/s11010-018-3401-1.

Kuo, Y.C., Lee, C.K., Lin, C.T., 2018. Improving sensitivity of a miniaturized label-free electrochemical biosensor using zigzag electrodes. Biosens. Bioelectron. 103, 130–137. https://doi.org/10.1016/j.bios.2017.11.065.

Lakshmipriya, T., Fujimaki, M., Gopinath, S.C.B., Awazu, K., Horiguchi, Y., Nagasaki, Y., 2013. A high-performance waveguide-mode biosensor for detection of factor IX using PEG-based blocking agents to suppress non-specific binding and improve sensitivity. Analyst 2863–2870. https://doi.org/10.1039/c3an00298e.

Lakshmipriya, T., Gopinath, S.C.B., Hashim, U., Tang, T.H., 2016. Signal enhancement in ELISA: biotin-streptavidin technology against gold nanoparticles. J. Taibah Univ. Med. Sci. 11, 432–438. https://doi.org/10.1016/j.jtumed.2016.05.010.

Larson, N.R., Wei, Y., Middaugh, C.R., 2018. Label-free, direct measurement of protein concentrations in turbid solutions with a UV–Visible integrating cavity absorbance spectrometer. Anal. Chem. 90, 4982–4986. https://doi.org/10.1021/acs.analchem.8b00502.

Lee, S.H., Choi, S., Kwon, K., Bae, N.H., Kwak, B.S., Cho, W.C., Lee, S.J., Jung, H. Il, 2017. A photothermal biosensor for detection of C-reactive protein in human saliva. Sens. Actuators B Chem. 246, 471–476. https://doi.org/10.1016/j.snb.2017.01.188.

Liu, C., Cai, H., Jia, J., Cao, T., Xu, C., Liu, C., 2017. Research on highly sensitive optomagnetic sensor for rapid detection of inflammation. Technol. Heal. Care 25, S151–S156. https://doi.org/10.3233/THC-171317.

Md Arshad, Khairuddin, M., Faris Bin Mohamad Fathil, M., C.B. Gopinath, S., Rahim Ruslinda, A., Nuzaihan Md Nor, M., Yoong Lam, H., Hashim, U., 2016. Cardiac biomarkers: invasive to non-invasive assessments. Curr. Med. Chem. 23, 4270–4284. https://doi.org/10.2174/0929867323666161004150857.

Pandit, S., Dasgupta, D., Dewan, N., Ahmed, P., 2016. Nanotechnology based biosensors and its application. Pharma Innov. J. TPI 5, 18–25.

Poongodi, G.L., Suresh, N., Gopinath, S.C.B., Chang, T., Inoue, S., Inoue, Y., 2002. Dynamic change of neural cell adhesion molecule polysialylation on human neuroblastoma (IMR-32) and rat pheochromocytoma (PC-12) cells during growth and differentiation. J. Biol. Chem. 277, 28200–28211. https://doi.org/10.1074/jbc.M202731200.

Pundir, C.S., Narwal, V., 2018. Biosensing methods for determination of triglycerides: a review. Biosens. Bioelectron. 100, 214–227. https://doi.org/10.1016/j.bios.2017.09.008.

Sharifi, M., Avadi, M.R., Dashtestani, F., Ghorchian, H., Rezayat, S.M., Saboury, A.A., 2018. Cancer diagnosis using nanomaterials based electrochemical nanobiosensors. Biosens. Bioelectron. https://doi.org/10.1016/j.bios.2018.11.026.

Thangamuthu, M., 2018. Label-free electrochemical immunoassay for C-reactive protein. Biosensors 8, 34. https://doi.org/10.3390/bios8020034.

Victor dos Santos Junior, C., Sader, M.S., Gonçalves, G.C., Weissmüller, G., Simão, R.A., 2018. Effect of pH on the adsorption and interactions of bovine serum albumin with functionalized silicon nitride surface. Colloids Surf. B Biointerfaces 167, 441–447. https://doi.org/10.1016/j.colsurfb.2018.03.045.

Xu, S., Zhang, R., Zhao, W., Zhu, Y., Wei, W., Liu, X., Luo, J., 2017. Self-assembled polymeric nanoparticles film stabilizing gold nanoparticles as a versatile platform for ultrasensitive detection of carcino-embryonic antigen. Biosens. Bioelectron. 92, 570–576. https://doi.org/10.1016/j.bios.2016.10.058.

Zubiate, P., Zamarreño, C.R., Sánchez, P., Matias, I.R., Arregui, F.J., 2017. High sensitive and selective C-reactive protein detection by means of lossy mode resonance based optical fiber devices. Biosens. Bioelectron. 93, 176–181. https://doi.org/10.1016/j.bios.2016.09.020.